

MARINE GRAVITY ANOMALY USING SATELLITE ALTIMETRY

AJIN RUFUS, KIRTHANA

ABSTRACT : Global sea surface heights (SSH) and gravity anomaly are computed on a $6^\circ \times 6^\circ$ from SARAL altika mission over the period of 2013-2016 at a region of Bay of Bengal. Altimetry data contain 35 cycle over the period of 3 years. The ascending and descending tracks were separated to reduce the computation. Only the descending tracks were taken. The Slope of along the track is calculated which gives the Deflection Of Vertical (DOV). From the calculated DOV the components ξ and η were at a regular grid interval. Then the grided DOV components are related to the gravity anomaly by using 2D Fast Fourier Transformation. The gravity anomaly from Jason-2 mission was also tried.

1. Introduction

With the gradual deepening of global exploration (Li,2019), the ocean surface has become a key feature for resource detection. The Gravity data over the ocean can describe the Earth with much accuracy since 70 % of Earth is covered by ocean and the geoid is the shape that is close to the Mean sea level. However the acquisition of gravity data over the marine is expensive and inefficient. In recent decades the satellite altimetry has become a mainstream approach (Wan,2018). Processing of Altimetry data can give the Sea surface height which is subtracted from Mean sea level to obtain geoid undulation. The geoid undulation can be inverted by any of the Least square collocation (Hofmann-wellenhof, 2006), inverse stokes (Yuan Fang,2021), inverse Hotine (Wan,2020) method, Fast fourier transform (Defu Che, 2021), to get gravity anomalies.

In this Fast fourier transform was used. This method is said to have comparatively high accuracy. The inverse of Fourier will result in gravity anomaly of the surface.

Gravity anomalies g can be obtained by:

$$g = F^{-1} \left\{ -l \frac{\gamma}{\text{mód } k} [k_x F(\eta) + k_y F(\chi)] \right\} \quad (1)$$

F is forward fourier and F^{-1} is the inverse fourier. l is the imaginary. k_x is the wave number in X-direction, k_y is the wave number in y-direction (Hwang and Parsons 1996).

2. Study Area and Data

2.1. Study area

The area taken is Bay of Bengal is 86 deg E, 13 degN to 92 deg E, 19 degN. The Altimetry data over the period of 3 years (2013-2016) have been obtained total 35 cycles.

2.2. Data

The altimetry Data of SARAL-Altika mission (Satellite with ARGOS and ALtiKa) a cooperative altimeter technology of ISRO and CNES, Launched at February of 2013 was obtained from Open Altimeter DataBase (OpenADB). SARAL increases the altimeter frequency for better range precision and shown outstanding performance in obtaining precise geoid and gravity fields (Raney and Phalippou 2011). The domain of measurement is Atmosphere and ocean which includes measurement of Ocean topography, Ocean surface winds, Ocean wave height and spectrum, and Atmospheric Humidity Fields. It measures ocean surface topography using a very high electromagnetic frequency Ka band of 35.75 GHz.

3. Methodology

In Altimetry the sea surface height is the distance between the satellite with respect to the reference ellipsoid and the ocean surface from the satellite. Figure 1 shows the Sea surface height that is measured by the satellite.

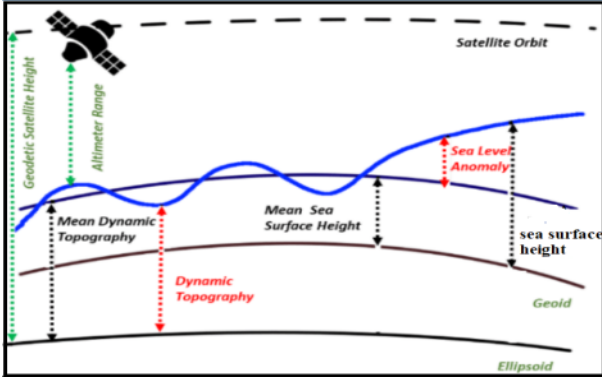


Figure 01: SSH of Satellite altimetry

The SARAL data were downloaded from OpenADB for the region of interest (Bay of Bengal) for the period of 2013-2016. It contains both ascending and descending tracks, in order to reduce the computation process the descending tracks alone separated and taken for the process. Each cycle has number of passes hence number of descending tracks were observed with a slightly deviation in position with one other. The median of the tracks was calculated per cycle to get one track per cycle. The local direction of gravity is normal to the geoid, and the angle between this direction and the normal to the ellipsoid is known as the deflection of the vertical. It is calculated by equation(2)

$$\frac{h_j - h_i}{s_{ij}} = \frac{\delta N}{\delta s} \quad (2)$$

and since,

$$DOV, \epsilon = -\frac{\delta N}{\delta s} \quad (3)$$

therefore, the DOV is computed by combining equations 2 and 3,

$$DOV, \epsilon = -\left(\frac{h_j - h_i}{s_{ij}}\right) \quad (4)$$

where, $s_{ij} = \delta s$ is the distance between two points δN is the height undulation. Since the distance between two DOV points is 6km (less than 12 km) the Mean Dynamic topographic Correction is neglected.

The DOV has two components east-west(η) and north-south(ξ) Figure 2 is given by.

$$\frac{\delta N}{\delta s} + \epsilon = \xi \cos \alpha + \eta \sin \alpha \quad (5)$$

where α is the azimuth is given by

$$= \arctan\left(\frac{\cos \phi_j \sin(\lambda_j - \lambda_i)}{\cos \phi_i \sin \phi_j - \sin \phi_i \cos \phi_j \cos(\lambda_j - \lambda_i)}\right) \quad (6)$$

Note that the ellipsoid used in the Saral-Altika, Jason 2 missions are the same that was used in TOPEX/Poseidon mission, which is the T/P ellipsoid having a semi major axis of 6378135.59 m and an inverse flattening value of 298.256999999994. In order to find the components of DOV the study region is divided into grid of $0.25^\circ \times 0.25^\circ$. The DOV components were found by the method Proposed by Defu Che et.al (2021). He used the indirect levelling method to find the components of DOV.

$$X = (A^T P A)^{-1} A^T P L \quad (7)$$

Where P is a weight matrix of inverse if the distance from the observation point to grid point. X is a column matrix of ξ and η and $L = (\epsilon(1) \dots \epsilon(n))^T$ The random is reduced by the relation

$$v = AX - L \quad (8)$$

The grid consist of atleast three value of DOV is selected and the grid without DOV is separated to do interpolation. Since there are only 7 track line it is interpolated so that each grid has a DOV.

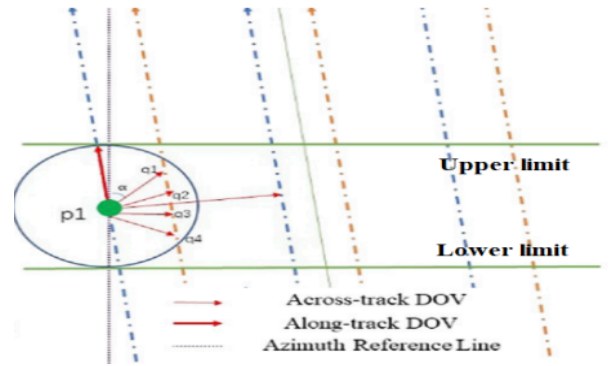


Figure 02: Components of DOV

Here scattered interpolation is used for interpolation as it is both simple and on the other hand gives values of high accuracy. The figure 03 shows the available (observed) DOV and Figure 04 shows that the DOV points needed to be interpolated

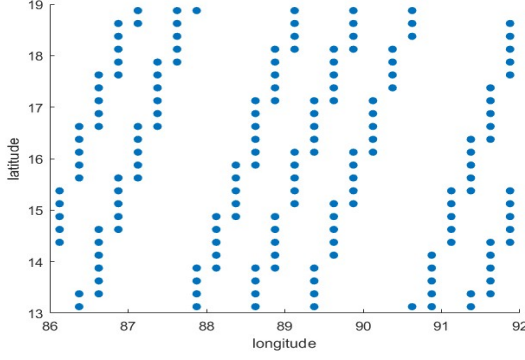


Figure 03: Available DOV

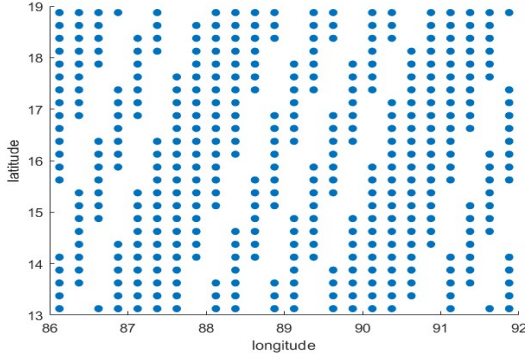


Figure 04: Non-Available DOV Components

After the interpolation normal gravity was calculated using Somigliana-Pizzetti Formula

$$\gamma = \frac{a\gamma(a)\cos^2\phi + b\gamma(b)\sin^2\phi}{\sqrt{a\cos^2\phi + b\sin^2\phi}} \quad (9)$$

Then the fast Fourier transform was carried out to find the gravity anomaly over the region. The fast Fourier involves the normal gravity that is given by Somigliana-Pizzetti Formula.

$$g = F^{-1}\left\{-l\frac{\gamma}{|k|}[k_x F(\xi) + k_y F(\eta)]\right\} \quad (10)$$

Where k_x is the wave number in x-direction, k_y is the wave number in y-direction and $|K| = \sqrt{k_x^2 + k_y^2}$

4. Results and Discussion

The ascending and descending tracks were separated shown in figure

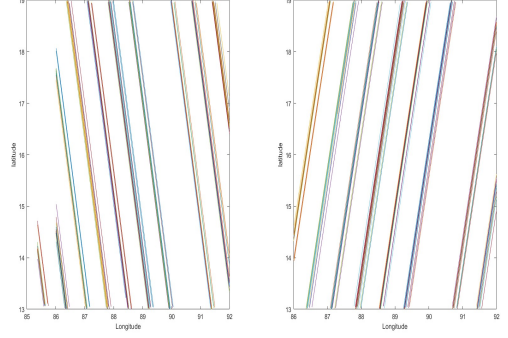


Figure 05: Ascending Descending tracks

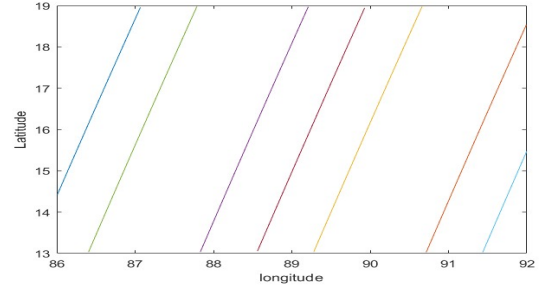


Figure 06: Median of Descending tracks

The slope of the points were calculated. The slope of the SSH is the Deflection of vertical at that point. The study area were divided into $0.25^\circ \times 0.25^\circ$ shown in Figure 07.

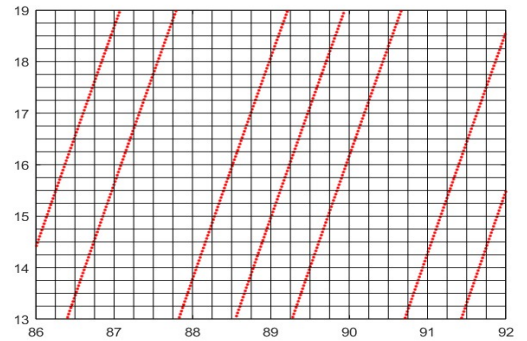


Figure 07: Gridded Area with DOV

The normal gravity also obtained for the region is shown in the figure below,

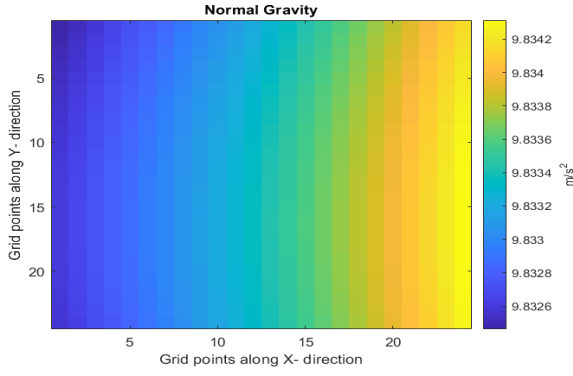


Figure 08:Normal Gravity

The number of DOV per grid varies from zero to four. So that the grid contains maximum of four DOV components. To fill the grids without DOV Scattering interpolation was used which ensures every grid has a DOV component. The visualisation of Gravity anomaly acquired after the 2-D FFT is shown in Figure 09.

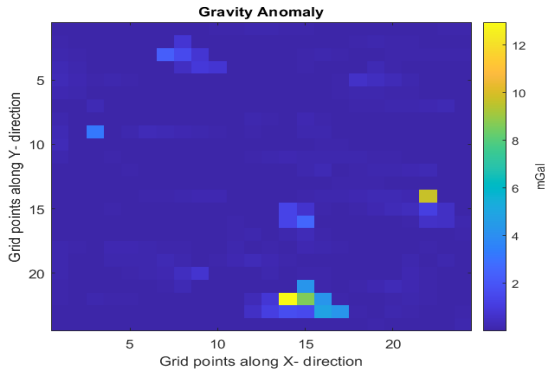


Figure 09:Gravity Anomaly

The gravity anomaly varies from -2 to $2.5 \times 10^{-6} \text{ms}^{-2}$. (-0.02 to $0.02 \mu\text{Gal}$). The gravity anomaly is almost even over the area. The maximum anomaly is found in the Eastern region which has the shorelines across the direction.

5. BONUS

Along with SARAL-Altika we tried to obtain the gravity anomaly over the area using the Jason-2 mission. The Sea surface Height obtained from Jason over 2013-2016 were shown in Figure 10.

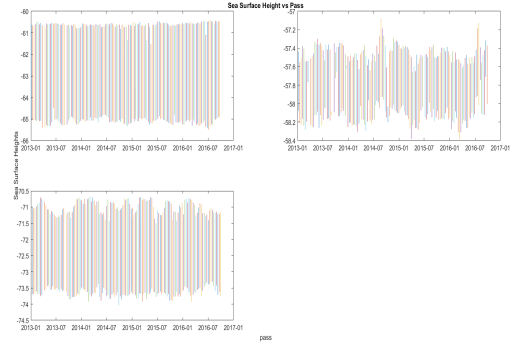


Figure 10:Sea Surface Height from Jason-2

The Same methodology was used to derive the gravity anomaly from Jason-2 . The results obtained from the Jason-2 were added below.

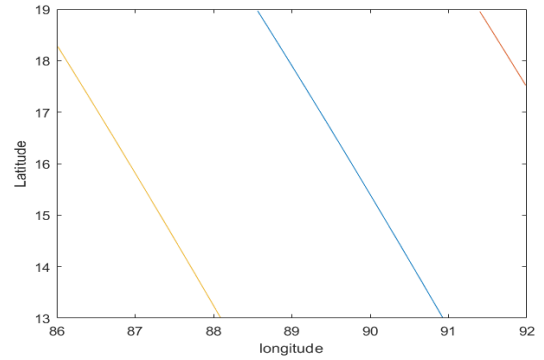


Figure 11:Mean Descending Tracks obtained from Jason-2

After taking the slope of Sea surface height the DOV were obtained.The whole area is grided into $0.25^\circ \times 0.25^\circ$.The number of DOV required to fill all grid (Figure 10) is greater than SARAL-Altika but number of available DOV per grid varied from 4 to 5 (Figure 12).

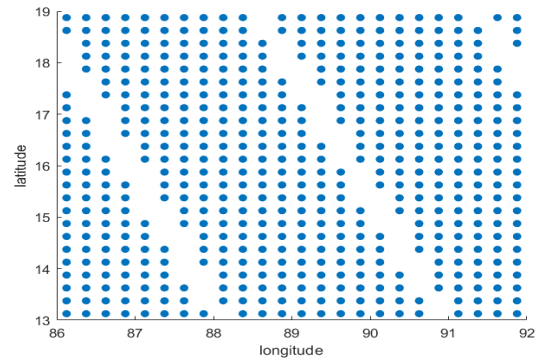


Figure 12:Points required (Not available DOV)

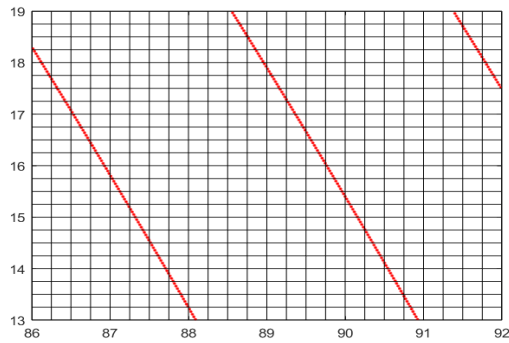


Figure 13:DOV obtained from SSH of Jason-2

Using the DOV values, the DOV components were found by following the method mentioned previously. Then, the normal gravity also obtained for the region shown in Figure 14

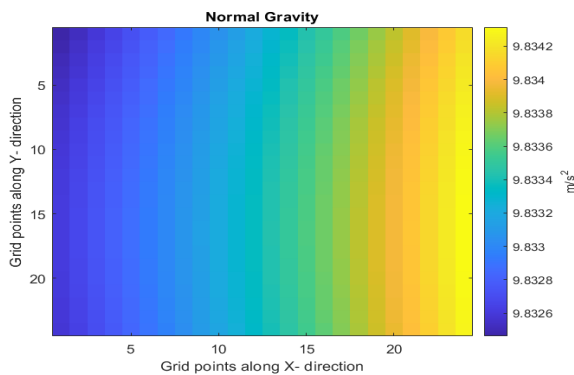


Figure 14: Normal Gravity

Finally the gravity anomalies are obtained and is shown in figure 15

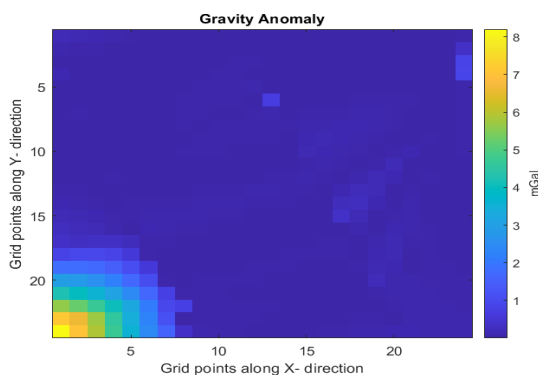


Figure 15:Marine Gravity Anomaly

6. References

- Che D, Li H, Zhang S and Ma B (2021) Calculation of Deflection of Vertical and Gravity Anomalies Over the South China Sea Derived from ICESat2 Data. *Front. Earth Sci.* 9:670256. doi: 10.3389/feart.2021.670256
- V.-S. Nguyen et al. / *Advances in Space Research* 66 (2020) 505-519. <https://doi.org/10.1016/j.asr.2020.04.051>
- Fang, Y.; He, S.; Meng, X.; Wang, J.; Gan, Y.; Tang, H. A Fast Method for Calculation of Marine Gravity Anomaly. *Appl. Sci.* 2021, 11, 1265. <https://doi.org/10.3390/app11031265>
- Hwang. C Hsu H.Y and Jang J.R .*Journal of Geodesy* (2002) 76: 407–418.:Global mean sea surface and marine gravity anomaly from multi-satellite altimetry: applications of deflection-geoid and inverse Vening Meinesz formulae. DOI 10.1007/s00190-002-0265
- Li, Y.; Guo, Q.; Huang, M.; Ma, X.; Chen, Z.; Liu, H.; Sun, L. Study of an Electromagnetic Ocean Wave Energy Harvester Driven by an Efficient Swing Body Toward the Self-Powered Ocean Buoy Application. *IEEE Access* 2019, 7, 129758–129769.
- Wan, X.; Ran, J. An alternative method to improve gravity field models by incorporating GOCE gradient data. *Earth Sci. Res. J.* 2018, 22, 187–193.
- Hofmann-Wellenhof, B.; Moritz, H. *Physical Geodesy*, 2nd ed.; Springer Vienna Publisher: Vienna, Austria, 2006.